Model Studies of Bearing Capacity and Failure Mechanism on Strip Footings Resting on Sand Slopes Utilizing the PIV Technique

Nabeel K. Lwti
Al-Furat Al-Awsat Technical University, Al-Najaf, Iraq
nabeelkl@atu.edu.iq (corresponding author)

Balqees A. Ahmed
Department of Civil Engineering, University of Baghdad, Baghdad, Iraq
balqees.a@coeng.uobaghdad.edu.iq

Received: 26 July 2025 | Revised: 20 August 2025 and 28 August 2025 | Accepted: 4 September 2025

 DOI: https://doi.org/10.48084/etasr.13663

ABSTRACT

The shallow foundations constructed near slopes alter the bearing capacity, creating challenges that are different from those on level ground. In addition, distinct deformations occur within the soil beneath the footing, associated with the resulting slope failure mechanism. This paper examines a series of small-scale physical modeling tests designed to investigate the bearing capacity behavior and failure mechanisms of strip footings placed on dry sand slopes. The model tests were conducted with varying setback distance ratios (D/B) and relative density conditions. The Particle Image Velocimetry (PIV) technique was utilized to monitor the soil distortion patterns and the progress of the failure surfaces during loading. According to the PIV analysis results, the failure mechanism of shallow footing near slopes is significantly influenced by the footing's position relative to the slope face. The results indicated that increasing the setback distance leads to a related linear rise in the ultimate bearing capacity (qu), with a critical setback distance ratio of D/B = 2, beyond which the influence of the slope becomes negligible at D/B ≥ 5. The failure surface geometry and displacement fields obtained from the PIV analysis closely reflect the transition from the bearing capacity failure to the slope stability failure. These findings highlight the role of setback distance and relative density on the footing performance near slopes. Furthermore, the application of PIV techniques proves to be a reliable and effective approach for observing the complex failure mechanisms, offering advantages over conventional theoretical methods.

Keywords-particle image velocimetry; strip footing; laboratory model; footing on sand slope; bearing capacity

I. INTRODUCTION

The research on footings located on sloping ground and the evaluation of the bearing capacity of shallow foundations near slopes are important issues. The critical factors that influence the stability of footings on sloped sites have been investigated, as they affect the design criteria of the entire footing slope system [1]. The bearing capacity of the footing may be significantly reduced depending on the latter's location with respect to the slope crest. Unlike the footings on level ground, those placed on sloping ground experience a reduced bearing capacity and potential slope instability [2-4]. A theoretical solution to determine the bearing capacity of a shallow footing embedded in or on the surface of the crest of a slope was proposed in [3]. Under ultimate loading, shear zones appear on the side of the slope, and the supporting capacity of the soil on that side significantly diminishes [5]. PIV is one of the most important laboratory techniques for assessing the soil distortion with small-scale physical models and capturing the immediate particle movement [6, 7]. In this research, model strip footing tests were conducted on sand for level ground and slope under stress-controlled conditions, to investigate the failure mechanism and bearing capacity. The objective is to obtain a broad understanding of the collapse mechanism for the strip footing near a sand slope and its influence on the bearing capacity and failure mode.

II. METHODOLOGY

A. Test Set-Up

The laboratory physical model tests were conducted in a steel tank with 0.5 mm thick walls and the following dimensions: 1,200 mm length, 462 mm width, 500 mm height. The strip footing (width B=70 mm) rests on the crest of the slope, parallel to the width of the tank, to simulate plane strain conditions. Its length is almost equal to the tank width. The front sidewall of the steel box was fabricated from 10 mm thick glass, as shown in Figure 1, to capture the movements of the

sand grains with a digital camera. Rough footing was made by supporting a thin layer of sand on the lower face with glue. A gap of 1 mm prevents the contact between the footing and the side walls. Vertical loads were applied to the model footings via a ball bearing by a hydraulic jack system. The loading rate was manually adjusted to 1.0 mm/min. An electronic load cell with a capacity of 5 kN was used to measure the applied loads. For settlement measurements, Linear Variable Displacement Transducers (LVDTs) are positioned at the two edges of the steel footing. The PIV technique used in this study provides a displacement measurement accuracy of approximately ±0.25 mm, consistent with previous research.

(a)

(b)

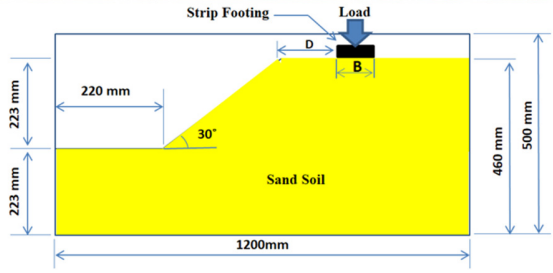

Fig. 1. (a) Experimental set-up used in this study and (b) schematic illustration of the slope geometry.

B. Ground Model

The sand was manually washed, air-dried, and categorized deploying the dry sieving method for particle size. Using the Unified Soil Classification System (USCS), it was classified as poorly graded sand (SP). The specific gravity of the soil particles was 2.65. The maximum and minimum dry densities for the sand were 18.95 and 16.43 kN/m³. In this study, depending on the packing technique, sand was placed in the model tank using the tamping method to achieve dense state conditions. The packing process involved storing the sand in 115 mm thick layers into the model container, starting with weighing the amount of the sand soil according to the dimensions for each layer. This procedure was necessary to build a particular relative density, depositing it in the model container and tamping it with a hand-held tool until obtaining the required level for each layer. The resulting density is 18.35 kN/m³, with a corresponding relative density of Dr = 79% and a friction angle of 37°, determined by the direct shear tests.

C. Test Program

The effects of various setback distance ratios (D/B) for strip footing on a sand slope were investigated, and the results for the slope case were compared with the level ground case. Two main groups of model tests were conducted under different test programs. First, the response of a strip foundation constructed on level ground was investigated. Second, a series of tests were carried out to study the behavior of a strip footing placed on sloping ground, focusing on its influence on the slope stability and failure mechanisms under vertical loading with other variables held constant. Table I provides a summary for all the test programs conducted for level ground and slope groups with the constant and variable parameters utilized.

TABLE I. TEST PROGRAM CONDUCTED FOR THE TWO GROUP TESTS

Group	Description	Variable parameters
1	Level ground tests, B=70 mm, Dr = 79%	-
2	Slope tests, β=30°, B=70 mm, Dr = 79%	D/B = 0, 1, 2, 3, 4, 5

D. Ultimate Bearing Capacity and Bearing Capacity Ratio

The ultimate bearing capacity (qu) is determined by the load settlement curve as the highest pressure on the foundation where soil failure occurs. The usual method for determining the load settlement curve is the allowable settlement method, which defines the ultimate bearing capacity depending on the limit value of the settlement, for example, 10% of B, where B is the width of the foundation [8-10]. The behavior of the bearing capacity can be represented by the non-dimensional bearing capacity reduction factor I_r for the footing on the sand slope as shown in [11]:

$$I_r = \frac{qu_{slope}}{qu} \quad (1)$$

where qu_{slope} is the ultimate bearing capacity of the footing on the slope and qu is the ultimate bearing capacity of the footing on the ground level.

III. DIGITAL IMAGING AND PIV TECHNIQUE

The concept of the PIV technique depends on capturing images of a targeted area and tracking the motion of individual particles in successive images. With the help of image processing software (GeoPIV program), the incremental worth of displacement and the strain can be determined. The PIV analysis was conducted using the MATLAB program to assess the failure mechanisms occurring during loading conditions. A Sony A7 III camera (full frame, 24 megapixels) facilitated the visualization of the soil movement during testing and image processing. The camera was positioned in front of the glass wall of the test container. The clarity of PIV depends on the patch size and the grid spacing. The strain estimation requires information on the variance of displacement across the successive images. Thus, the PIV analysis necessitates the choice of the optimal patch range that offers higher precision [12].

IV. RESULTS AND DISCUSSION

A. Experimental Results

The experimental results (Table II) demonstrate that the ultimate bearing capacity behaves linearly by increasing its value when the setback is increased, and the PIV analysis monitored and confirmed this behavior. The study demonstrates that when positioned at the slope crest of a setback distance of D/B=0 and then moved away from the slope face to a setback distance of D/B=2, there is an average value of 66% increase in the bearing capacity. After that, the increase rate diminishes. However, with a setback ratio of D/B=5, the bearing capacity on slope is the same as on level ground. This means that the effect of the slope is insignificant when the footing is situated at a setback distance bigger than five times the width of the footing, in the case of a 79% relative density. Similarly, the I_r values vary approximately linearly with the setback distance. For instance, the I_r achieved for the footing model tests positioned at a setback distance ratio of D/B = 0 showed an approximate 60% lower value to those at D/B = 5. The bearing capacity can be further improved with an increase of the relative density Dr. It is also noted that combining the relative density and setback distance effects can significantly improve the bearing capacity of the footing [13]. This observation is similar to the mode indicated in [3].

TABLE II. RESULTS OF QU AND I_R FOR FOOTING ON SLOPE WITH DIFFERENT SETBACK DISTANCE RATIOS

Relative density (Dr)	Setback distance ratio (D/B)	qu (KPa)	I_r %
79%	Level ground test	62.5	-
	0	16.5	0.24
	1	19.3	0.29
	2	27.6	0.41
	3	42.9	0.64
	4	67.4	0.99
	5	67.7	1

The curve of the load settlement for the level ground tests is illustrated in Figure 2, and for the sand slopes, with varying setback distance ratios, in Figure 3. The calculated bearing capacity reduction factor (I_r) values are displayed in Figure 4 and are in close agreement with those reported in [11, 14].

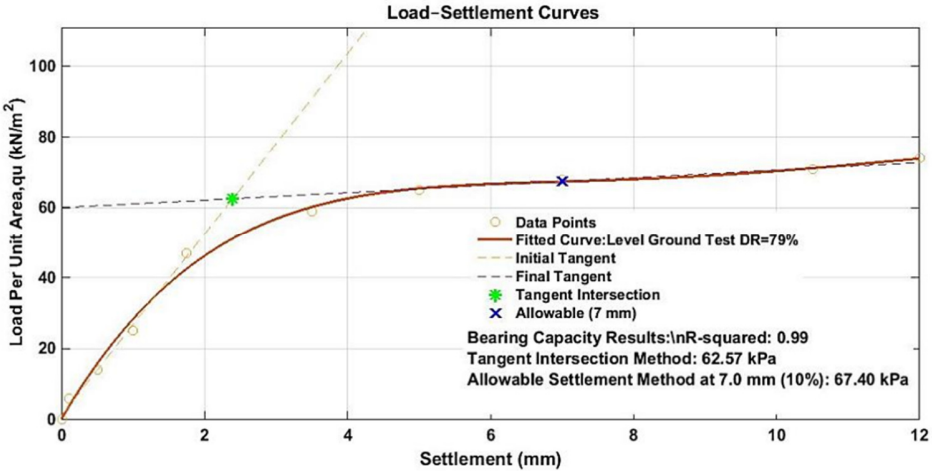

Fig. 2. Load-settlement curve for level ground with relative density Dr= 79%.

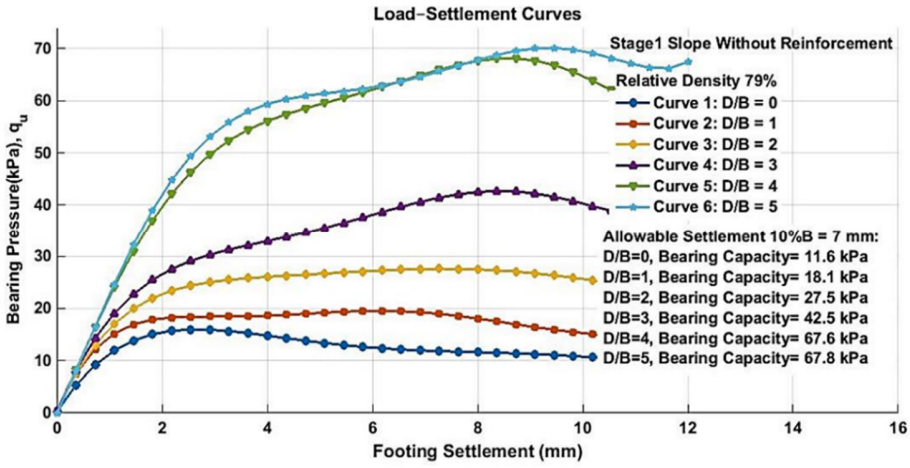

Fig. 3. Load–settlement curves at different D/B ratios and relative density Dr= 79%.

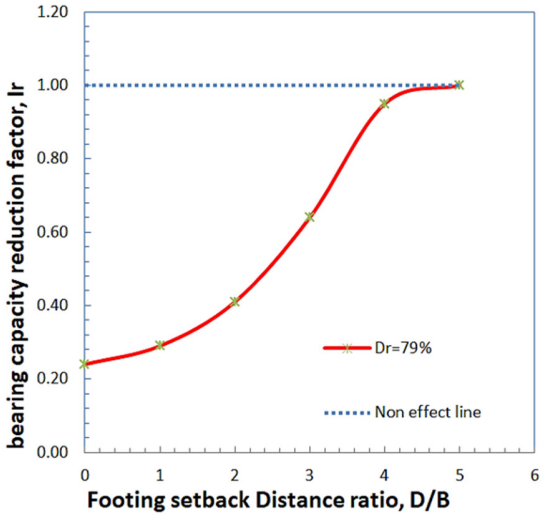

Fig. 4. Bearing capacity reduction factor for different footing setback distance ratios.

B. Failure Mechanism by PIV

The PIV analysis is utilized to assess the displacement and shear strain. The conventional assumption that the settlement is positive in the graphical output labeling was used. The vertical displacement plots have positive contours that indicate settlement and negative contours that indicate heave. In the horizontal displacement plots, the positive contours indicate rightward movement, and the negative contours indicate leftward movement. The laboratory image presented in Figure 5 captures the failure under applied pressure of the foundation with a zero setback distance. Taken during testing, it illustrates the development of the failure mechanism, and provides direct visual evidence of the deformation and slip surface formation. It also complements the PIV analysis, offering a clearer understanding and validation of the observed interaction between the soil and foundation.

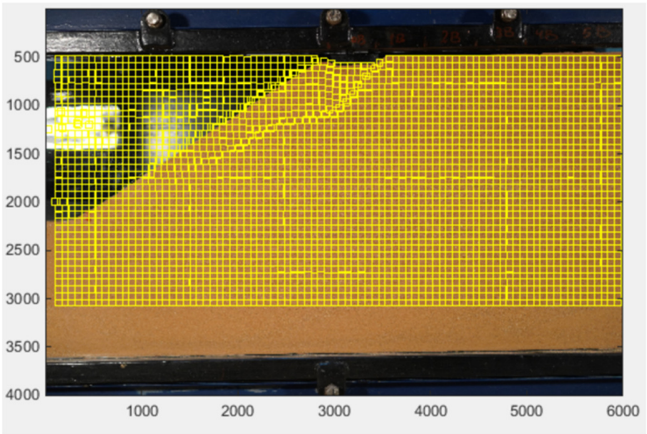

Fig. 5. The laboratory image presenting the development of the failure mechanism.

For the level ground case, Figure 6 shows the boundaries of the failure zones resulting from changing the applied stress on the footing from q=0 kPa to q=70 kPa, up to the allowable settlement of 10%B. The shear strain displayed in Figure 6c, which represents the high density, demonstrates a shear zone that extends laterally up to 2B from the footing and reaches the soil surface, consistent with the first type of bearing capacity failure known as general shear failure. It is observed that the effect of the footing extends vertically to a depth of 2B, and the horizontal effect extends to a distance of 3B from both sides of the footing. The behavior observed in the dense sand aligns with model predictions from earlier studies, such as [15].

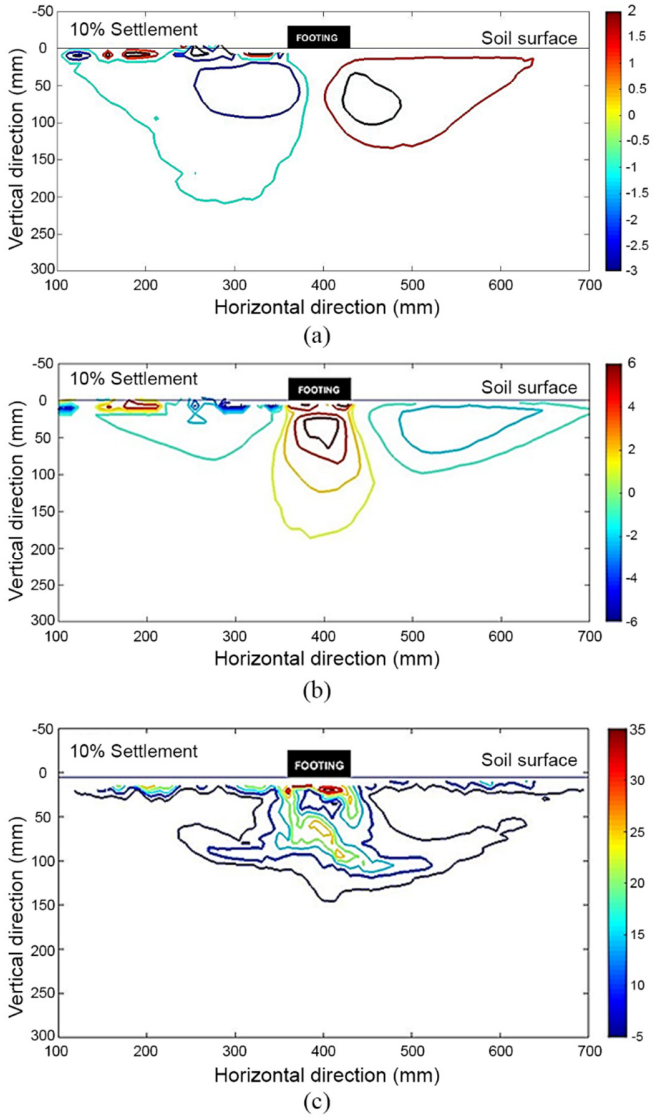

Fig. 6. Loading disturbance for strip footing resting on level ground sand soil to settlement of 10%B, with relative density 79%: Horizontal (a) and vertical (b) displacement in mm, shear strain (c) in %.

For the slope case, Figures 6 and 7 present the failure observed in the experimental tests for the bearing capacity. The literature points out that the failure region under the foundation is partitioned into active, passive, and radial shear zones. Notably, the traditional shear mechanism that guides the bearing capacity of the footing is greatly dependent on the

wedge angles formed on both sides of the active failure zone beneath the footing. On level ground, these angles tend to be symmetric, whereas on sloped ground, they become asymmetric [1]. The shape of the failure zone under the footing base on the slope body is demonstrated. The impact of the setback distance on the failure mechanism and, therefore, the bearing capacity for the case of a slope, and three setback distance ratios of 0, 2, and 5 are also exhibited. The failure mechanisms of unreinforced sand slopes can be investigated using numerical analysis, as proposed in [16], where the results indicated the presence of a critical zone directly underneath the footing. Outside this zone, there is no significant effect on the bearing capacity.

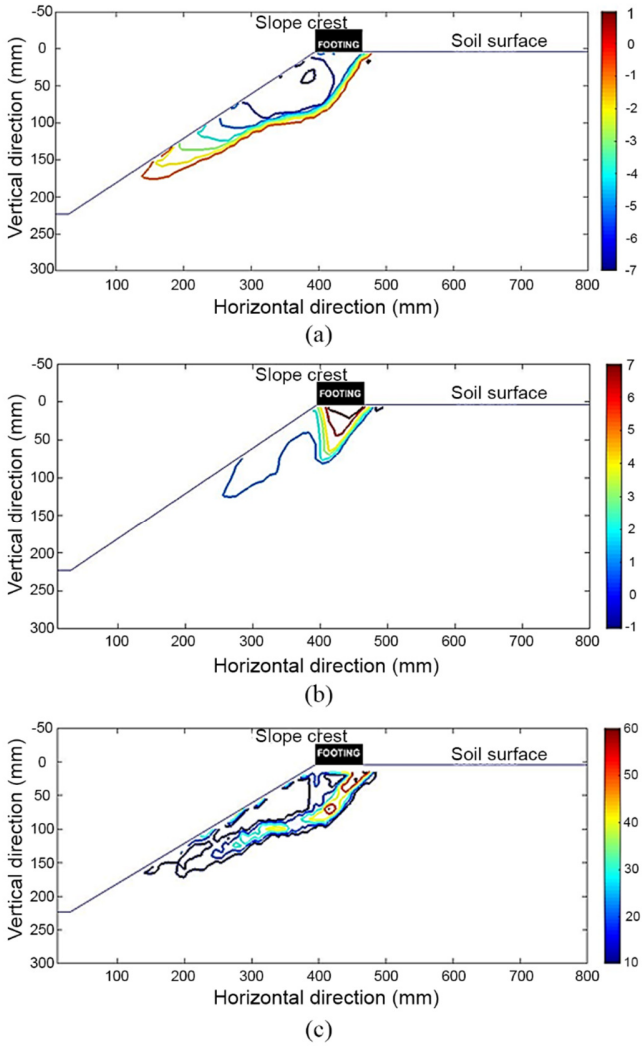

Fig. 7. Loading disturbance for strip footing resting on slope crest to settlement of 10%B, with relative density 79% and edge distance ratio of D/B=0 (Test 130): Horizontal (a) and vertical (b) displacement in mm, shear strain (c) in %.

For a relative density of 79% and setback D/B=0, the ultimate bearing pressure touches 12.10 kPa at a settlement of 1.5 mm and starts to drop with cumulative settlement. For setback distance ratios of D/B=2-D/B=5, the ultimate bearing pressure reaches the peaks of 29.83 kPa and 68.79 kPa at settlements of 1.75 mm and 3 mm, respectively, and begins to decrease. Moreover, the slip failure surface at a setback distance ratio of D/B=0, 1, initiating from the edge corner of the footing and propagating to the slope surface, leads to a complete loss of passive resistance as the load gradually increases. The footing collapses once an entirely developed shear failure of the slip occurs. Consequently, the soil starts moving laterally to the sloping edge.

The results shown in Figure 7 for a setback distance ratio of D/B=0, exhibit a higher lateral deformation than the level ground case. For a setback distance ratio of D/B=2-5, the soil shows less lateral deformation to the sloping side. Figures 7(c) and 8(b) illustrate a total maximum shear strain of 60% and 30%, respectively. It is observed that the value of the shear strain begins to decrease with an increasing setback distance for 10% allowable settlement. For the tests with a setback distance ratio of D/B=0, when the relative densities increased, the value of the shear strain generated by the loading began to disappear with the same allowable settlement due to the increased resistance of the soil to shear. If the footing is located at a setback distance ratio of D/B=1 or more, the length of the sliding surface increases, and the bearing capacity gradually comes closer to that for level ground.

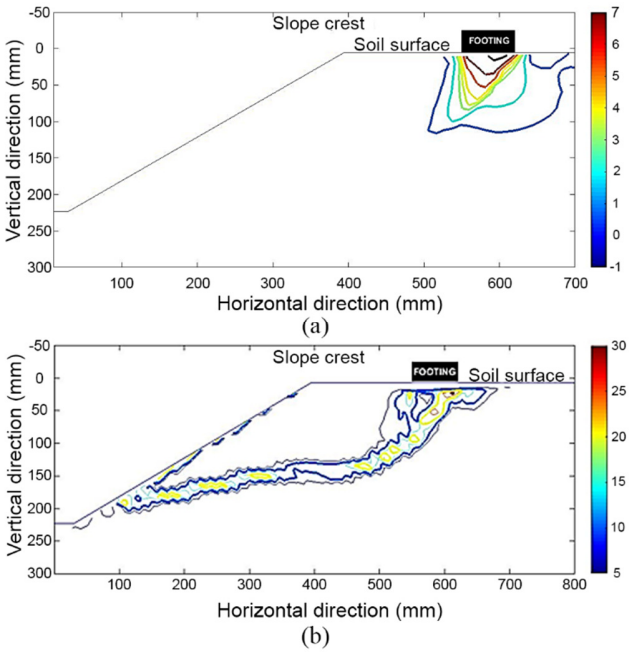

Fig. 8. Loading disturbance for strip footing resting on slope crest to settlement of 10%B, with relative density 79% and edge distance ratio of D/B=2 (Test 132): Vertical (a) displacement in mm, shear strain (b) in %.

The 79% relative density results are in excellent agreement with those reported in [9-11]. Furthermore, the PIV analysis shows that the mobilized shear strength of the soil is heavily dependent on the stress level, as proposed in [15] for the failure on sandy soil.

C. Transition of Failure Mode

For the level ground, the failure mode was transformed into the local shear failure with increased settlement because of the sand becoming denser after the loading process continued. This is attributed to the progressive densification and rearrangement of the sand particles during loading. The presence of the slope leads to the "sudden jerks" phenomenon, which includes successive collapses and is amplified by increasing the soil density. As shown in Figures 7 and 8, with a setback distance of D/B =3 or more, the footing-slope system behavior remains mainly controlled by bearing capacity mechanisms. Conversely, at a setback distance ratio of less than D/B=2, the slope significantly affects the stability of the footing.

At a setback ratio of D/B=2, the failure surface propagates toward the slope face, resulting in a face failure mode due to reduced passive resistance. On the contrary, when the setback ratio increases to D/B=3, the failure surface extends toward the slope toe, producing a toe failure mode. In this case, the bearing capacity decreases due to inadequate soil support beneath the footing. These findings emphasize the critical role of the setback distance, as greater distances promote a conventional bearing capacity behavior, whereas smaller distances accelerate the transition to slope-related failure mechanisms.

The findings of the present study are consistent with those of [17], where it was reported that the slope stability and footing performance improve with an increasing setback distance ratio, reaching a critical value at e/B≈3 beyond which the impact stabilizes. Furthermore, the bearing capacity increases significantly with a relative density of about 70%. Similarly, the experimental results using PIV analysis confirm this behavior: the bearing capacity rises notably with an increasing setback distance, with the most pronounced changes observed up to D/B=2 after which the rate of improvement decreases. Likewise, the tests performed at Dr=79% show the same trend, validating that the critical density observed in previous studies applies to the footing–slope systems examined in this study.

V. CONCLUSIONS

The investigation of the slope-footing system used in this study combines traditional bearing capacity failure and the slope stability failure mechanism. The results show that the setback distance ratio is the most important factor that influences the bearing capacity of the shallow foundation on the slope. An increase in the setback distance ratio leads to a comparable increment in both the bearing capacity and the bearing capacity reduction factor (I_r) of the model footing. The critical setback distance ratio is D/B=2. Further than this value, the bearing capacity increases linearly up to a setback distance ratio of D/B=5 and then stabilizes, similar to that for the footing located on level ground. The most common failure mode was the bearing capacity failure. However, a setback distance ratio less than D/B=2 demonstrates the slope stability failure mechanism. The load–settlement curve behavior for footing on a slope reveals two distinct modes: peak load resistance and a "sudden jerk" phenomenon. The peak load resistance is noticed in the case of 79% relative densities. The occurrence of "sudden jerks" is inherent in all cases and is attributed to the influence of the slope.

REFERENCES

[1] B. Leshchinsky and Y. Xie, "Bearing Capacity for Spread Footings Placed Near c′-ϕ′ Slopes," *Journal of Geotechnical and Geoenvironmental Engineering*, vol. 143, no. 1, Jan. 2017, Art. no. 06016020, https://doi.org/10.1061/(ASCE)GT.1943-5606.0001578.

[2] E. B. Altalhe, M. R. Taha, and F. M. Abdrabbo, "Behavior of strip footing on reinforced sand slope," *Journal of Civil Engineering and Management*, vol. 21, no. 3, pp. 376–383, Feb. 2015, https://doi.org/10.3846/13923730.2014.890646.

[3] G. Meyerhof, "The ultimate bearing capacity of foundations on slopes," in *4th International Conference on Soil Mechanics and Foundation Engineering*, London, 1957, pp. 384-386

[4] S. K. Dash, N. R. Krishnaswamy, and K. Rajagopal, "Bearing capacity of strip footings supported on geocell-reinforced sand," *Geotextiles and Geomembranes*, vol. 19, no. 4, pp. 235–256, May 2001, https://doi.org/10.1016/S0266-1144(01)00006-1.

[5] H. Khalvati Fahliani, M. R. Arvin, N. Hataf, and A. Khademhosseini, "Experimental Model Studies on Strip Footings Resting on Geocell-Reinforced Sand Slopes," *International Journal of Geosynthetics and Ground Engineering*, vol. 7, no. 2, May 2021, Art. no. 24, https://doi.org/10.1007/s40891-021-00270-1.

[6] B. A. Ahmed and D. A. R. Al-Hamdani, "Investigation of the Deformation of Sandy Soil Near a Laterally Loaded Single Pile Using the Particle Image Velocimetry Technique," in *Current Trends in Geotechnical Engineering and Construction*, Singapore, 2023, pp. 178–194, https://doi.org/10.1007/978-981-19-7358-1_16.

[7] H. M. Jawad and Z. K. Jahanger, "Collapse Pattern in Gypseous Soil using Particle Image Velocimetry," *IOP Conference Series: Earth and Environmental Science*, vol. 1374, no. 1, Aug. 2024, Art. no. 012012, https://doi.org/10.1088/1755-1315/1374/1/012012.

[8] F. Ashkan and H. Sadighi, "Numerical and laboratory investigation of effect of soil reinforcement on settlement of strip foundations," *Journal of Geology and Mining Research*, vol. 12, no. 4, pp. 107–117, Oct. 2020, https://doi.org/10.5897/JGMR2020.0347.

[9] G. M. Latha and A. Somwanshi, "Bearing capacity of square footings on geosynthetic reinforced sand," *Geotextiles and Geomembranes*, vol. 27, no. 4, pp. 281–294, Aug. 2009, https://doi.org/10.1016/j.geotexmem.2009.02.001.

[10] Y. Xu, G. Yan, D. J. Williams, M. Serati, A. Scheuermann, and T. Vangsness, "Experimental and numerical studies of a strip footing on geosynthetic-reinforced sand," *International Journal of Physical Modelling in Geotechnics*, vol. 20, no. 5, pp. 267–280, Apr. 2019, https://doi.org/10.1680/jphmg.18.00021.

[11] M. Salih Keskin and M. Laman, "Model studies of bearing capacity of strip footing on sand slope," *KSCE Journal of Civil Engineering*, vol. 17, no. 4, pp. 699–711, May 2013, https://doi.org/10.1007/s12205-013-0406-x.

[12] D. Lesniewska and D. M. Wood, "Observations of Stresses and Strains in a Granular Material," *Journal of Engineering Mechanics*, vol. 135, no. 9, pp. 1038–1054, Sept. 2009, https://doi.org/10.1061/(ASCE)EM.1943-7889.0000015.

[13] B. S. Albusoda and L. A. K. Salem, "Bearing Capacity of Shallow Footing Resting on Dune Sand," *Journal of Engineering*, vol. 18, no. 03, pp. 298–308, Mar. 2012, https://doi.org/10.31026/j.eng.2012.03.02.

[14] A. Cerato and A. Lutenegger, "Scale effects of shallow foundation bearing capacity on granular material," in *BGA International Conference on Foundations, Innovations, Observations, Design and Practice*, Dundee, 2003, pp. 217–225.

[15] A. S. Vesić, "Analysis of Ultimate Loads of Shallow Foundations," *Journal of the Soil Mechanics and Foundations Division*, vol. 99, no. 1, pp. 45–73, Jan. 1973, https://doi.org/10.1061/JSFEAQ.0001846.

[16] B. Mazouz, T. Mansouri, M. Baazouzi, and K. Abbeche, "Assessing the Effect of Underground Void on Strip Footing Sitting on a Reinforced Sand Slope with Numerical Modeling," *Engineering, Technology &*

Applied Science Research, vol. 12, no. 4, pp. 9005–9011, Aug. 2022, https://doi.org/10.48084/etasr.5131.

[17] E. Baah-Frempong and S. K. Shukla, "Stability analysis and design charts for a sandy soil slope supporting an embedded strip footing," *International Journal of Geo-Engineering*, vol. 9, no. 1, p. 13, Sept. 2018, https://doi.org/10.1186/s40703-018-0082-2.